Indian Journal of Chemistry
Vol. 63, July 2024, pp. 678-684
DOI: 10.56042/ijc.v63i7.7521

Molecular interaction and dielectric relaxation study of DMSO-water binary mixtures using a TDR

Aniket D Bokhare[a], Nitin P Garad[b], Milind P Lokhande[a] & Ashok C Kumbharkhane*[b]

[a] Department of Physics and Electronics, Govt. Vidarbha Institute of Science and Humanities, Amravati 444 604, MS, India

[b] School of Physical Sciences, Swami Ramanand Teerth Marathwada University, Nanded 431 606, MS, India

E-mail: akumbharkhane@yahoo.co.in

Received 23 December 2023; accepted (revised) 27 June 2024

Complex permittivity spectra (CPS) for dimethylsulphoxide (DMSO) - Water mixtures, in the frequency range of 10 MHz-30 GHz have been examined, which include the entire concentration range using a time domain reflectometry (TDR) method. The Cole - Davidson relaxation model has been used to fit the CPS obtained from DMSO - Water mixtures. Mixture's relaxation time obtained high at volume fraction of water, Vw = 0.3. The study analyzes the intermolecular interactions using the Kirkwood correlation factor (KCF) and excess properties. The theoretical dielectric constant for mixtures has been computed using Alenka Luzar's hydrogen bonding model using different molecular parameters.

Keywords: Hydrogen bonding, Relaxation time, Intermolecular interaction, Permittivity

Dielectric Relaxation spectroscopy (DRS) has made important advances to our knowledge of the dynamics of systems over the past decades. DRS's broad frequency range can be used to learn in-depth details about specific motional processes, whose timescales can range from 10^{-12} seconds to 10^{3} seconds. This study also demonstrates how this knowledge complements the known properties of the same materials using related relaxation and spectroscopic techniques[1]. DRS can help us to better understand the properties of relevant liquid mixtures in solutions[2]. DRS is more beneficial as it measures how a sample's dipole moment changes in response to an electric field, to observe the collective motion of a molecular ensemble[3].

DMSO, a widely used solvent in laboratories, is renowned for its high solvent power due to its high polarity, hydrogen bond (H-bond) formation ability, and its ability to remain liquid at various temperatures[4]. DMSO has a number of pharmacological applications[5,6]. It is a polyfunctional molecule containing two hydrophobic CH_3 groups and a strongly polar hydrophilic S=O group[7]. DMSO aqueous solutions are particularly interesting due to their distinctive biological and physiochemical characteristics[8]. According to the findings of molecular dynamics, DMSO and water molecules typically create two H-bonds. The variation in H-bond lifetime between DMSO-Water and water-water interactions is attributed to the unique properties of DMSO, which allow it to form stronger and more stable H-bonds with water molecules compared to water-water interactions[9]. Alenka Luzar has suggested a classical model for an H-bonded mixture to investigate the excess dielectric characteristics of different compositions of DMSO-Water mixtures[10].

Iwona Powas *et al.* studied the dielectric spectra of the DMSO + water mixture and suggested that the static permittivity on the composition of the DMSO and water combinations somewhat deviates from linearity[11]. For DMSO aqueous solutions at 25°C, U. Kaatze *et al.* determined the CPS throughout the whole composition range between 1 MHz and 40 GHz. They took measurements of the static permittivity, which suggests that the dipole moments are ordered antiparallel[2]. Understanding the structural characteristics of DMSO-water combination, particularly at low concentrations, according to Kaatze *et al.* is still a matter of debate[2]. This is the reason for studying these solutions, specifically at low DMSO concentration, in our present work. By conducting experiments and analyzing the data, we aim to contribute to the understanding of the H-bond structural properties of DMSO aqueous solutions at low concentrations. The study investigated complex permittivity in the 10 MHz to 30 GHz frequency range, determining static dielectric constant (ε_0) and

relaxation time (τ) using the least squares fit method. The excess dielectric permittivity and KCF were also determined for DMSO-water binary mixtures. The study compares theoretical and experimental values of ε_0 using Alenka Luzar's hydrogen bonding model.

Experimental Section

Materials

DMSO was purchased commercially and allowed for its direct use without additional purification. The water was chosen as a solvent. The binary mixture of DMSO and water was prepared in various volume fraction of water in DMSO.

Measurements

We used the TDR to determine CPS of the DMSO-water mixture using a Tektronix digital serial analyzer, specifically model DSA8300 sampling mainframe oscilloscope. Sampling module 80E10B provided precise measurements and analysis capabilities for the time domain reflectometer. Fig. 1 shows the TDR block diagram, which illustrates the components and connections used in the TDR technique. This diagram provides an overview of how the TDR technique is implemented and the equipment involved. A 12 ps incident and 15 ps reflected rising time pulse are provided by the sampling module. These pulses which are reflected pulse without sample, denoted as $R_1(t)$ and with sample, denoted as $R_x(t)$ were recorded in a time window of 5 ns and digitized in 2000 points as shown in Fig. 2. The coaxial cable used has 50-ohm impedance. The CPS was determined through the Fourier transformation of reflected pulses and data analysis previously[12,13].

Results and Discussion

Complex Permittivity Spectra

Fig. 3 shows frequency dependent CPS for DMSO-Water at various concentrations obtained by TDR in the frequency range from 10 MHz to 30 GHz at 25°C.

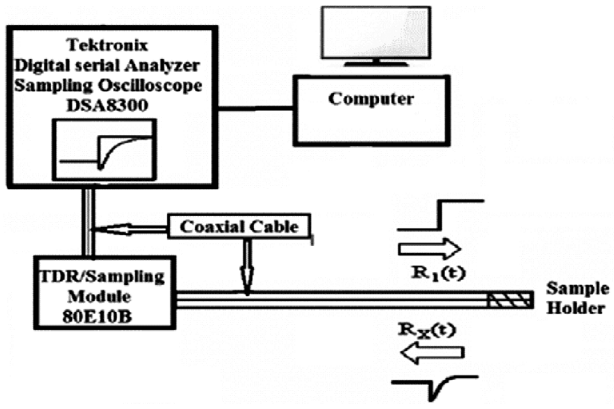

Fig. 1 — Time Domain Reflectometry (TDR) Block Diagram.

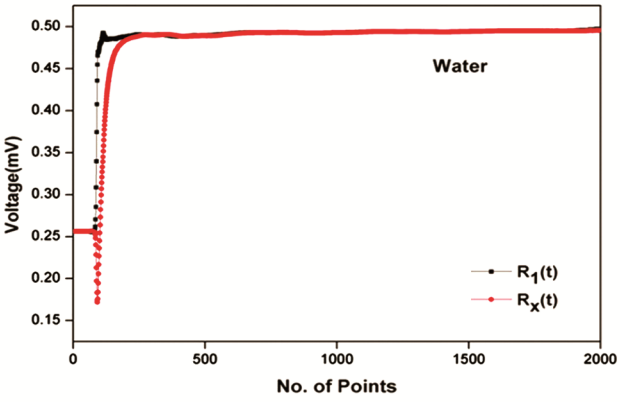

Fig. 2 — TDR Waveform: Reflected pulses with and without Sample.

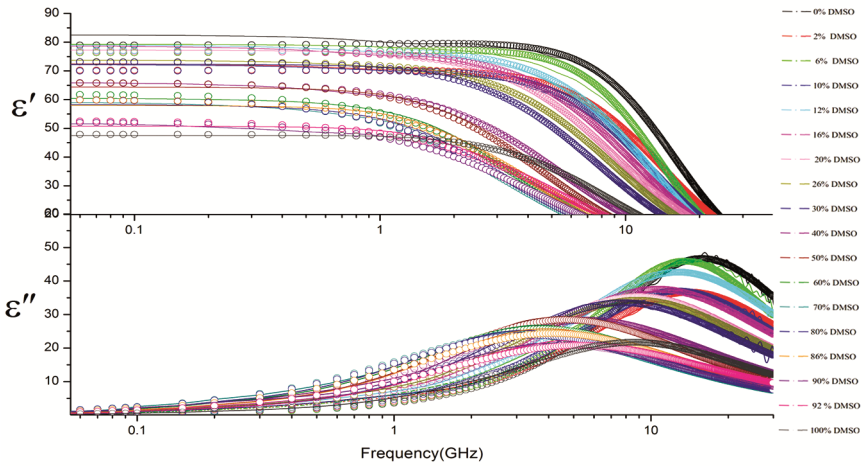

Fig. 3 — Frequency dependence dielectric complex permittivity spectra for DMSO + Water mixture for various concentrations at 25°C.

This shows that dielectric permittivity decreases as frequency increases, indicating dielectric dispersion. This behaviour is typical for polar liquids like DMSO-Water, where the dipole relaxation processes become more dominant at higher frequencies.

Static Dielectric Constant

The experimentally measured CPS using TDR is fitted to Havriliak – Negami(H-N) formula[14,15].

$$\varepsilon^*(\omega) = \varepsilon_\infty + \frac{\varepsilon_0 - \varepsilon_\infty}{[1+(j\omega\tau)^{1-\alpha}]^\beta} \quad \ldots (1)$$

where ε_0 , τ, ε_∞ , α and β are fitting parameters. H-N expression involves three different models: Debye (α =0, β = 1)[16], Cole-Cole ($0 \leq \alpha \leq 1$ and $\beta = 1$)[17] and Davidson – Cole ($\alpha = 0$ and $0 \leq \beta \leq 1$)[18]. Table 1 displays dielectric parameters for DMSO-Water mixtures at various temperatures. This shows that the ε_0 value for DMSO-Water mixtures decreases from water to DMSO. It implies that adding DMSO to water reduces the polarity of the mixture, and the ε_0 value decreases as well. This is because DMSO disrupts the H-bonding network of water. When DMSO is added to water, it can displace the water molecules from each other, breaking the H-bonds. This reduces the polarity of the mixture and the ε_0 value. But at low concentrations of DMSO, ε_0 value for DMSO-Water mixtures significantly decreases. Possibility is that the DMSO molecules are able to aggregate at low concentrations. This would decrease the number of water molecules available to make hydrogen bonds, lowering the polarity of the mixture and the ε_0 value.

Dielectric relaxation time

Table 1 reveals that the relaxation time in the DMSO-Water mixture decreases with an increase in temperature. At small DMSO content, values of dielectric relaxation time increase with X_{DMSO}. Mixture's relaxation time is high at concentration 0.7 DMSO. However, the dielectric relaxation time reduces from 0.7 DMSO to pure DMSO. This reduction in τ can be attributed to the increased mobility of the DMSO molecules at higher concentrations. The high concentration of DMSO allows for more efficient dipole rotation, resulting in a shorter relaxation time compared to pure DMSO.

Kirkwood correlation factor

Kirkwood-Frohlich equation (KFE) is a tool used to measure the degree of dipole orientation resulting from H-bond interactions in pure liquids. The dipole orientation is measured by the g value, which deviates from unity. Theoretical static dielectric constant can be determined using the KFE as given below[19]:

$$\frac{(\varepsilon_0 - \varepsilon_\infty)(2\varepsilon_0 + \varepsilon_\infty)}{\varepsilon_0(\varepsilon_\infty + 2)^2} = gi\mu^2 \frac{4\pi N\rho}{9kTM} \quad \ldots (2)$$

where ε_0= static dielectric constant, *i*=1 and 2 refers to water and DMSO, respectively, M stands for molecular weight, μ_i refers to dipole moment of water

Table 1 — Dielectric parameters: a) Dielectric constant (ε_0) b) relaxation time (τ) for DMSO-Water mixture

Temp.	25°C		20°C		15°C	
V_{DMSO}	ε_0	τ(ps)	ε_0	τ(ps)	ε_0	τ(ps)
0	78.92(13)	10.07(02)	79.1(11)	10.98(02)	80.2(09)	11.35(01)
0.02	70.19(09)	11.29(02)	70.96(08)	11.89(02)	71.41(12)	14.08(03)
0.06	76.29(20)	11.68(04)	78.55(11)	11.46(02)	79.9(33)	12.68(06)
0.1	69.96(11)	12.56(03)	71.91(05)	12.55(01)	73.48(19)	13.86(05)
0.12	76.99(08)	12.44(01)	77.7(08)	13.09(01)	79.82(09)	13.89(02)
0.16	76.8(07)	14.92(02)	77.47(13)	15.36(03)	79.25(17)	16.21(05)
0.2	76.79(09)	17.7(03)	77.41(09)	18.23(03)	79.24(07)	19.61(03)
0.26	73.21(04)	17.9(19)	74.8(03)	19.11(01)	77.6(05)	20.42(02)
0.3	73.18(16)	20.39(07)	73.79(04)	21.55(02)	76.32(06)	23.17(03)
0.4	66.00(06)	28.31(05)	67.17(05)	29.35(04)	69.03(09)	32.13(08)
0.5	65.9(09)	34.00(09)	67.17(11)	35.25(11)	68.17(13)	39.22(15)
0.6	61.9(11)	42.13(16)	62.09(12)	43.82(17)	63.67(15)	48.01(24)
0.7	60.34(14)	49.00(24)	60.35(19)	50.64(35)	61.58(24)	55.49(50)
0.8	60.2(14)	46.97(25)	60.55(16)	51.71(31)	61.96(22)	58.48(48)
0.86	60.1(14)	38.0(19)	60.50(16)	42.9(25)	61.09(20)	49.10(36)
0.9	52.25(10)	36.77(25)	53.25(10)	35.59(14)	55.07(16)	37.74(24)
0.92	52.7(13)	30.11(15)	53.2(13)	32.93(17)	54.58(18)	35.49(26)
1	47.9(01)	18.50(01)	47.91(02)	20.42(01)	49.41(02)	20.81(02)

Numbers in bracket denotes uncertainties in the last significant digits obtained by the least square fit method. *e.g.* 78.92(13) means 78.92 ± 0.13

and DMSO molecule which represents the separation of positive and negative charges within a molecule, ρ_i is density, Avogadro's number is indicated by N, g_i is the KCF for the i^{th} liquid component, kT has usual meaning. ε_∞ refers to dielectric constant at high frequency. Dielectric phenomena are exceedingly difficult to understand in terms of the KCF for a mixture composed of associated compounds. Hence it is necessary to make assumptions in order to calculate the average correlation factors g_1 and g_2 from a single value of ε_0.

Theoretical ε_0 calculated using KCF offers a more comprehensive understanding of the mixture's properties. Luzar proposed a theoretical model for H-bonded mixtures[10]. The following equations are used to calculate 'g_1' and 'g_2'.

$$g_1=1+Z_{11}\cos\varphi_{11}+Z_{12}\cos\varphi_{12}\,(\mu_2/\mu_1) \quad \ldots (3)$$

$$g_2=1+Z_{21}\cos\varphi_{21}\,(\mu_1/\mu_2) \quad \ldots (4)$$

where the average angles between neighboring dipoles of water and DMSO molecules are denoted by φ_{11}, φ_{12} and φ_{21}. The average number of H-bond with Water-Water, Water-DMSO and DMSO-Water pairs are $Z_{11} = 2 < n^{11}{}_{HB} >$, $Z_{12} = <n^{12}{}_{HB}>$, and $Z_{21} = <n^{21}{}_{HB}>\ (1\text{-}V_{water})/V_{water}$ respectively. The volume fraction of water is denoted by V_{water}. The g_1 and g_2 for various Water-DMSO mixtures at 25°C are determined and are plotted in Fig. 4. The values deviate from the ideality, which confirms that the H-bond complications overall impact on the dipolar ordering of the mixture's components.

The average number of H-bonds $\langle n_{HB}^{11}\rangle$, $\langle n_{HB}^{12}\rangle$ and $\langle n_{HB}^{21}\rangle$ per water molecule for 1i pairs (i =1 or 2) has been evaluated using[10]:

$$\langle n_{HB}^{11}\rangle = n_{1i}\omega^{1i}/n_1 \quad \ldots (5)$$

where number density of water molecules is indicated by n_1. The possibility of H-bond creation between water and DMSO is represented by equation $\omega^{1i} = 1/[1+ \alpha^{1i} \exp(\beta E^{1i})]$. $\beta = 1/kT$. Statistical volume ratios of the two sub-volumes of the phase space associated with the H-bonded and non-H-bonded pairs are indicated by α^{1i}. E^{11} and E^{12} indicate energy levels for 11 and 12 pair respectively. The number of densities of the H-bonded pairs between water and DMSO (n_{12}) and between Water-Water molecules ($n_{11}= 2n_1 - n_{12}$) gives the values of $\langle n_{HB}^{12}\rangle$ and $\langle n_{HB}^{11}\rangle$ respectively[10].

Fig. 5 shows that $\langle n_{HB}^{12}\rangle$ decreases and $\langle n_{HB}^{11}\rangle$ increases when water content increases. When the water concentration is low, each water molecule has a higher chance of forming an H-bond with DMSO molecule as compared to another water molecule. As the water concentration increases, there are more water molecules than DMSO molecules. This means that each water molecule has a higher chance of forming a H-bond with another water molecule than with a DMSO molecule.

The average number of H-bonded $\langle n_{HB}^{11}\rangle$, $\langle n_{HB}^{12}\rangle$ and $\langle n_{HB}^{21}\rangle$water-DMSO pairs $[n^{12}{}_{HB}]_V$ per unit volume (/cm^3) was determined by Eq.6[20]:

$$\left[n_{HB}^{12}\right]_V = \frac{V_{water}N}{M_{water}} n_{HB}^{12}\ (/cm^3) \quad \ldots (6)$$

where V_{water} is volume fraction of water, N denotes Avogadro number and M_{water} indicates molecular weight of water. Fig. 6 represents $[n^{12}{}_{HB}]_V$ *versus* V_{water}. The value of $[n^{12}{}_{HB}]_V$ found to be a maximum at $V_{water} \approx 0.3$.

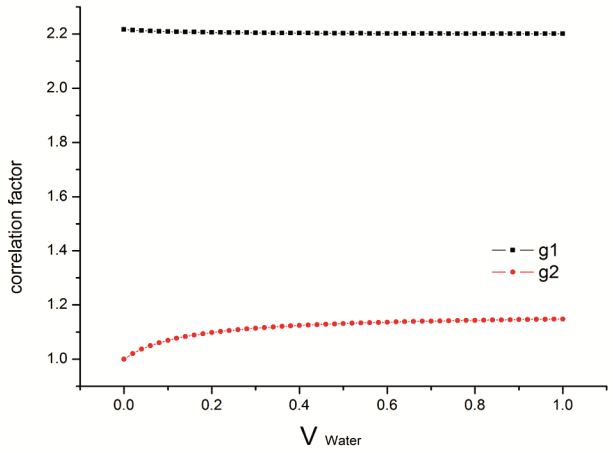

Fig. 4 — Plots of the correlation factor g_1 & g_2 *vs* V_{water}.

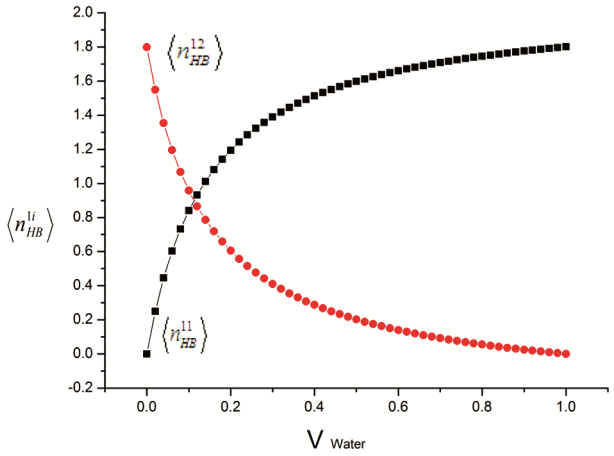

Fig. 5 — Plots of the average number of H-bonds between Water - Water molecule (n11 pair) and Water-DMSO (n_12 pair) *vs* Vwater

Table 2 displays the best possible molecular parameter values in our analysis. The comparison of theoretical and experimental values of ε_0 for Water-DMSO mixtures is provided in Fig. 7.

We also investigated how molecular parameters influence the ε_0 value using the Luzar model. We determined the theoretical values of the ε_0 for the three distinct values of the dipole moment of water and plotted them against the $V_{water,}$ as shown in Fig. 8. The plot clearly indicates a positive correlation between the ε_0 and the volume fraction of water. Additionally, we observed that as the dipole moment of water increased, the ε_0 also increased, suggesting a stronger polarization effect. The value of the ε_0 did not change significantly at low water concentrations. This suggests that the presence of water has a minimal effect on the ε_0 at low concentrations. However, as the water content increased, the ε_0 showed a noticeable increase, indicating a stronger influence of water on the polarization of the mixture.

We calculated the theoretical values of the ε_0 for the three values of number of H- bonds and plotted them against the V_{water}, as represented in Fig. 9. This

Table 2 — Molecular parameters used for determining ε_0

Dipole moment[a] of Water	2.07
Dipole moment[a] of DMSO	4.2
Polarizibility[b] for Water	1.5
Polarizibility[b] for DMSO	8
Bonding energy[c] for Water- Water	–13.7
Bonding energy[c] for Water- DMSO	–15
Enthalpy[c] of DMSO -DMSO	28
Enthalpy[c] of Water-Water	48

[a]Unit: Debye; [b]Unit : A^{03}; [c]Unit: kJ/mol

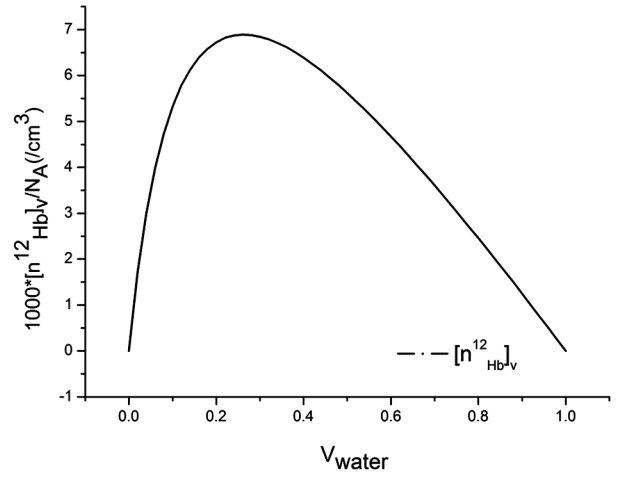

Fig. 6 — Plots of the number of H- bonds per unit volume against V_{water}.

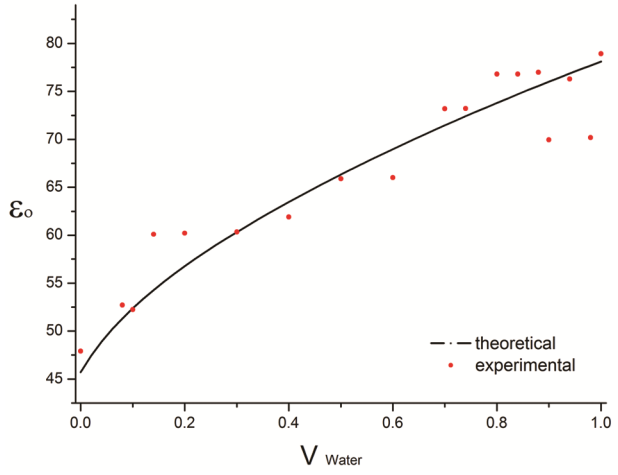

Fig. 7 — Comparison of experimental and theoretical values of ε_0 *vs* V_{water} at 25°C.

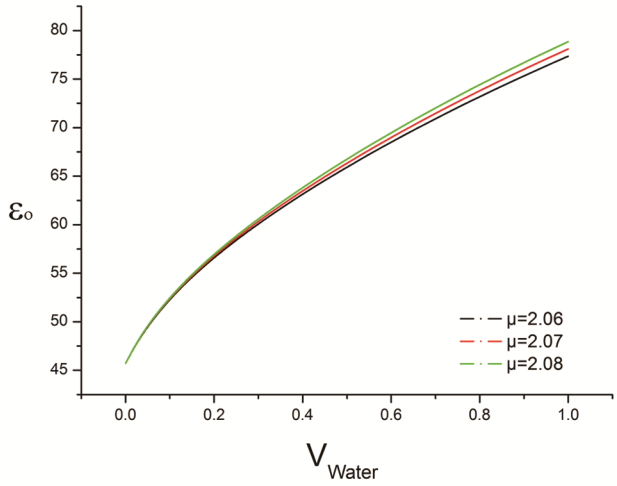

Fig. 8 — Theoretical values of ε_0 against Volume fraction of Water (V_{water}) for the three distinct values of the dipole moment of water at 25°C.

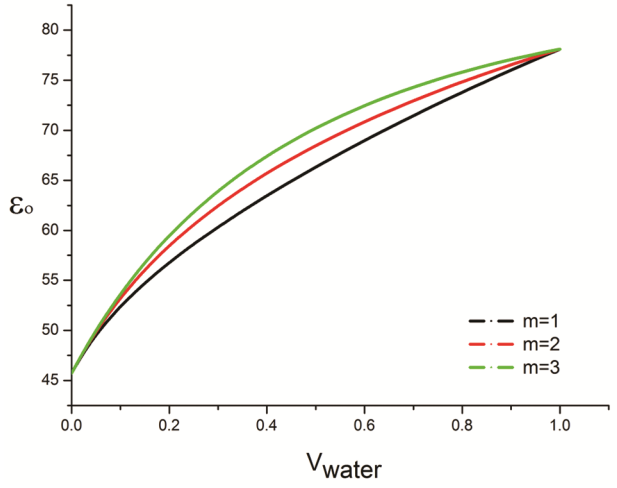

Fig. 9 — Theoretical values of ε_0 against Volume fraction of Water (Vwater) for the three distinct values of number of H-bond at 25°C.

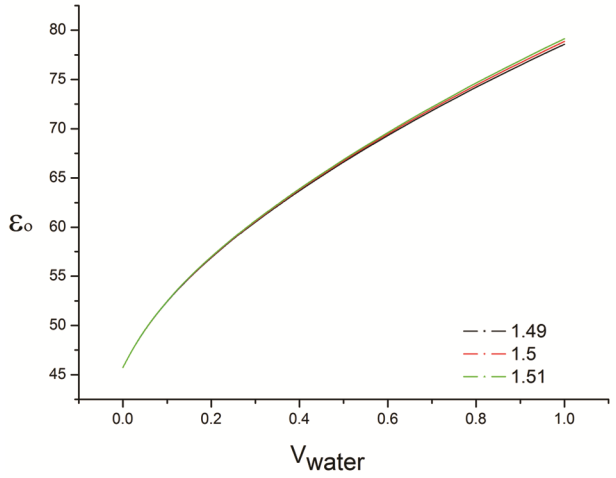

Fig. 10 — Theoretical values of ε_0 against V_{water} for three distinct values of polarizability of water at 25°C.

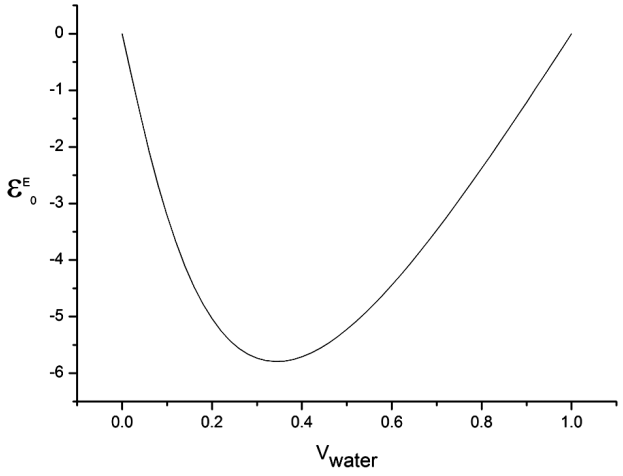

Fig. 11 — Excess permittivity *vs* V_{water} at 25°C temperature.

reveals that an increase in H-bonds leads to a higher dielectric constant. Finally, we calculated the theoretical values of the ε_0 for the three different values of the polarizability of water and plotted them against V_{water}, as shown in Fig. 10. At low water content, there was no appreciable change in the dielectric constant, while there was a substantial change at high water content.

Excess static dielectric constant ($\varepsilon_0{}^E$)

The Luzar model is utilized to study the impact of H-bonding on dielectric characteristics of mixtures, using $\varepsilon_0{}^E$. The $\varepsilon_0{}^E$ is expressed as:

$$(\varepsilon_0)^E = (\varepsilon_0)_M - \left[\frac{(\varepsilon_0)_{water}\, V_{water} + (\varepsilon_0)_{DMSO}}{(1 - V_{water})}\right] \quad \ldots (7)$$

where V_{water} - volume fraction of water and suffices M, water and DMSO represents mixture, solvents and solute, respectively.

The graph of $\varepsilon_0{}^E$ *vs*. V_{water} at 25°C represented in Fig. 11 indicates a negative value of $\varepsilon_0{}^E$, suggesting the tendency of mixture to form larger structures, known as multimers, through H-bonding. These multimers have a reduced effective dipole moment, which affects the dielectric properties of the mixture[21,22]. It is found that $\varepsilon_0{}^E$ for DMSO-water mixture exhibits a maximum negative deviation at 0.3 water content. It suggests that at this specific composition, there are particularly strong attractive interactions between DMSO and water molecules, resulting in a lower permittivity than expected. These interactions may involve H-bonding intermolecular forces which impact on ε_0 of the mixture.

Conclusions

The study reveals that H-bonding is formed in DMSO-water binary mixtures, as indicated by the dielectric parameters, excess parameters, and KCF. The experimental measured ε_0 agrees with the theoretical static ε_0 values determined using the Luzar model. It is not always possible to predict how solute-solvent molecules will interact and affect the ε_0 of a mixture because of their complex nature. These interactions can cause deviations from expected behavior and result in a ε_0 that is either higher or lower than predicted.

Acknowledgement

Author AD Bokhare would like to thank the Director of the G.V.I.S.H. in Amravati. The author of this work expresses sincere appreciation to the School of Physical Sciences at SRTM University in Nanded (MS) for providing laboratory facilities. Additionally, the author would like to extend gratitude to the SARTHI, Pune, for a fellowship (CSMNRF-2021). This fellowship provided valuable financial support and allowed the author to concentrate on the research without worrying about financial constraints. We kindly acknowledge the financial support provided by the Department of Science and Technology (DST), New Delhi (Project number: DST PROJECT-SB/S2/LOP-032/2013).

References

1 Kremer F & Schönhals A, *Broadband Dielectric Spectroscopy*, (Springer, Science & Business Media) 2002.

2 Kaatze U, Pottel R & Schäfer M, *J Phy Chem,* 93 (1989) 5623.

3 Markarian S A & Gabrielyan L S, *Phys Chem Liq*, 47 (2009) 311.
4 Martin D, Weise A & Niclas H-J, *Angew Chem Int Ed Engl*, 6 (1967) 318.
5 Ingrid E, Nakamura H, Lam V, Hofs E, Cederberg R, Cait J, Hughes M R, *PLoS One,*11 (2016) e0152538.
6 Santos N C, Figueira-Coelho J, Martins-Silva J & Saldanha C, *Biochem pharmacol*, 65 (2003) 1035.
7 Zijie L, Evangelos M, Macdonald D D & Lanagan M, *J Phys Chem A*, 113 (2009) 12207.
8 Vaisman I I & Berkowitz M L, *J Am Chem Soc*, 114 (1992) 7889.
9 Alenka Luzar & Chandler D, *J Chem Phys*, 98 (1993) 8160.
10 Alenka L & Stefan J, *J Mol Liq*, 46 (1990) 221.
11 Iwona P, Swiergiel J & Jadzyn J, *J Chem Eng Data*, 58 (2013) 1741.
12 Bokhare A D, Garad N P, Lokhande M P & Kumbharkhane A C, *Phy Chem Liq,* 62 (2024) 1.
13 Kumbharkhane A C, Puranik S M & Mehrotra S C, *J Chem Soc Faraday Trans*, 87 (1991) 1569.
14 Havriliak S & Negami S, *J Poly Sci C Poly Symp*, 14 (1966) 99.
15 Sarode A V & Kumbharkhane A C, *J Mol Liq,* 160 (2011) 109.
16 Debye P, *Pressure Broadening and Debye's Relaxation Equation Polar molecules*, (New York: Chemical Catalog) 1929.
17 Cole K S & Cole R H, *J Chem Phys*, 9 (1941) 341.
18 Davidson D W & Cole R H, *J Chem Phys*, 18 (1950) 1417.
19 Kirkwood J G, *J Chem Phys,* 7 (1939) 911.
20 Seiichi S, Oshiki N, Shinyashiki N, Yagihara S, Kumbharkhane A C & Mehrotra S C, *J Phys Chem A*, 111 (2007) 2993.
21 Baliram L & Madhurima V, *J Mol Model*, 17 (2011) 709.
22 Sengwa R J, Sankhla S, & Shinyashiki N, *J Sol Chem*, 37 (2008) 137.